Article

Combining α-Al$_2$O$_3$ Packing Material and a ZnO Nanocatalyst in an Ozonized Bubble Column Reactor to Increase the Phenol Degradation from Wastewater

Adnan K. Majhool, Khalid A. Sukkar *[ID] and May A. Alsaffar

Department of Chemical Engineering, University of Technology-Iraq, Al-Sanna St., Baghdad 19006, Iraq;
che.21.11@grad.uotechnology.edu.iq (A.K.M.); may.a.muslim@uotechnology.edu.iq (M.A.A.)
* Correspondence: khalid.a.sukkar@uotechnology.edu.iq

Abstract: The ozonation reaction in a bubble column reactor (BCR) has been widely used in the removal of phenol from wastewater, but the phenol removal efficiency in this type of reactor is limited because of low ozone solubility and reactivity in the system. In the present study, the phenol degradation in the BCR was enhanced by using α-Al$_2$O$_3$ as a packing material and a ZnO nanocatalyst. The reactor diameter and height were 8 cm and 180 cm, respectively. The gas distributor was designed to include 52 holes of a 0.5 mm diameter. Also, the gas holdup, pressure drop, and bubble size were measured as a function of the superficial gas velocity (i.e., 0.5, 1, 1.5, 2, 2.5, and 3 cm/s). The evaluation of the hydrodynamic parameters provided a deeper understanding of the ozonation process through which to select the optimal operating parameters in the reactor. It was found that the best superficial gas velocity was 2.5 cm/s. A complete (100%) phenol removal was achieved for phenol concentrations of 15, 20, and 25 ppm at reaction times of 80, 90, and 100 min, respectively; this was achieved by using α-Al$_2$O$_3$ packing material and a ZnO nanocatalyst in the BCR. Additionally, a reaction kinetics study was conducted to describe the ozonation reaction in BCR. The first-order reaction assumption clearly describes the reaction kinetics with an R^2 = 0.991. Finally, the applied treatment method can be used to efficiently remove phenol from wastewater at a low cost, with a small consumption of energy and a simple operation.

Keywords: phenol removal; multiphase reactor; ozone gas; removal efficiency; reaction mechanism

1. Introduction

The production of high-quality water is one of the primary targets of environmental sustainability. This can be achieved using an efficient treatment process for industrial wastewater to provide a healthy ecosystem [1–3]. All industrial wastewater treatment processes focus on reducing waste-producing pollutants. Managing the treatment processes of wastewater and effluent is the key factor in providing a high-performance treatment process. Most petroleum refineries and petrochemical plants produce a high range of hydrocarbons in wastewater [4–7]. All of these materials cause fatal problems for humans and the environment. Phenol is one of these dangerous chemicals that is produced within effluent wastewater, and it requires efficient treatment techniques to be removed [8–10]. The hydrocarbon materials can be removed from wastewater using various industrial reactors, such as membrane reactors, fluidized bed reactors, trickle bed reactors, and bubble column reactors (BCRs). BCRs are one of the most applied gas–liquid and gas–liquid–solid multiphase reactors in industrial processes. They are characterized by many benefits such as easy operation, efficient mixing, high heat and mass-transfer rates, low maintenance costs, and low energy consumption [11–15].

In a BCR, the movement of bubbles inside the reactor induces liquid mixing (i.e., effective hydrodynamic performance) so that high mass transfer and heat transfer can be achieved. Additionally, the evaluation of the hydrodynamic behaviors of the bubble

column reactor will determine the extent of a chemical reaction, as well as the reactor's performance [16]. The main hydrodynamic parameters in a BCR are the reactor height-to-diameter ratio, superficial gas velocity, gas holdup, bubble size, gas–liquid interfacial area, flow patterns, and gas distributor design [17–21]. The use of bubble columns in wastewater treatment is highly dependent on the mass-transfer mechanism between the gas and liquid phases. Thus, understanding the operational parameters of the diffusion process will provide a clear picture, delineating an effective process for the removal of hydrocarbons in a BCR [4,22]. The degradation of various hydrocarbon contaminants from the effluent streams of wastewater that employ BCRs must provide effective contact between the reaction mixtures. The degradation process of hydrocarbons occurs in the liquid phase, and gas bubbles encourage an efficient mass transfer with the pollutant materials included in the system before the oxidation reaction [23–26].

The addition of packing materials inside a BCR will enhance the reaction mechanism due to the increased contact surface area between the gas and liquid phases [8,27]. Therefore, a high chemical reaction rate will be achieved with a short residence time. The packing material supports the formation of a thin film over the packing surfaces. This thin film is characterized by a low resistance to mass transfer such that a high chemical reaction rate can be attained. Moreover, the ozonation reaction kinetics indicate that the chemical reaction usually produces hydroxyl radicals [21,26]. These free radicals are highly volatile in the reaction media in converting organic material (e.g., phenol) into simple compounds (e.g., water and carbon dioxide) [28–33]. Furthermore, the flow regime inside the BCR plays a critical role in determining the reactor's performance. Due to the difficulty of predicting the flow behavior in a BCR, evaluation of the superficial gas velocity can contribute to the determination of the flow patterns, as well as the exact hydrodynamic behavior. Therefore, more extensive work is needed to reveal the relationship between the gas–liquid–solids in a BCR in terms of removing phenol from wastewater [34–41].

Ghaisani et al. [42] applied a semicontinuous, multi-injection BCR in the degradation of phenolic compounds when in the presence of ozone gas. They achieved the highest removal efficiency of 99.48 and 99.83% via ozonation and catalytic ozonation methods, respectively, which were conducted at an operating time of 60 min. Also, they indicated that the degradation process was highly influenced by the activity of hydroxyl radicals in the reactor. Wei et al. [43] used a rotating packed bed reactor in the presence of a Fe–Mn–Cu/γ–Al$_2$O$_3$ catalyst to enhance phenol removal from wastewater, and this was 96.42% effective at 30 min. Al-Ezzi [44] employed a pulsed BCR and loop reactor to treat phenol by using activated carbon as an adsorbent media in the reactor, and they found that around a 90% phenol removal efficiency was achieved. Honarmandrad et al. [45] investigated the reaction of phenol in wastewater in the presence of CaO$_2$ and ozone as the gas phase. They noted that the chemical reaction was endothermic with the highest reaction yield being 97.8% for a synthetic sample of wastewater at 90 min. Jothinathan et al. [46] treated petrochemical wastewater via an ozonation process in the presence of an Fe/GAC catalyst in micro-bubble and macro-bubble operations. They noted that the highest chemical oxygen demand (COD) removal efficiency was 88%, which was 18 and 43% greater than the micro-bubble and macro-bubble ozonation reactions, respectively. Alattar et al. [47] studied the removal of phenol from wastewater using an ozonized packed BCR, finding a removal efficiency of 100% of phenol after 30 min. This study showed that the packing material was a key factor in increasing the contact surface area between the gas and liquid phases, which also affected the phenol degradation rate. Bhosale et al. [48] evaluated the scale-up requirements of ozonation reactors to remove the phenolic compounds from wastewater. From the results of the reaction kinetics analysis, the authors noted that the reaction rates of the phenolic compounds were highly influenced by the mass-transfer mechanism and ozonation reaction.

The literature demonstrates that it is still difficult to understand how the hydrodynamic parameters influence the mass-transfer mechanism in a BCR when using ozone gas in the presence of packing materials. Also, the ozonation reaction usually exhibits poor

solubility and a fast decomposition of the ozone molecules [14,30]. All of these factors provide limited mass transfer in the liquid-phase reaction inside a BCR. Hence, it is necessary to identify the various superficial ozone gas velocities and evaluate their effect on the reactor's performance [47–54]. Therefore, the main objective of the present work is to enhance the ozonation reaction to attain a high phenol removal from the wastewater when using an ozonized packed BCR, as well as to evaluate the influence of the hydrodynamic behavior and packing material on the reactor's performance.

2. Materials and Methods

2.1. Materials

Many chemicals were utilized in the experiential runs, including the phenol compound (C_6H_5OH, 99.8% purity), which was purchased from (Thomas Baker Co. Ltd., Mumbai, India), as well as sodium thiosulfate (99.86% purity), potassium iodide (99.42% purity), and sulfuric acid (99.55% purity), which were obtained from (BDH Co. Ltd., London, UK). Moreover, α-Al_2O_3 was used as a packing material and ZnO NPs were used as the nanocatalyst, and both were purchased from (Sigma-Aldrich Co. Ltd., St. Louis, MO, USA).

2.2. Reaction Apparatus

The reaction apparatus consisted of a packed bubble column reactor (BCR). The reactor operated in fed-batch mode, in which the liquid phase (i.e., polluted wastewater) was stationary, while the gas phase (i.e., ozone gas) entered the reactor continuously in the upward flow direction. All of the treatment experiments were achieved at a constant operating temperature of 25 °C. The interaction between the gas phase and the liquid phase produced gas bubbles depending on the applied superficial gas velocity and other hydrodynamic parameters. These ozone bubbles were highly dispersed in the wastewater inside the reactor. Figure 1 illustrates the schematic diagram of the reaction apparatus of a BCR. The system contained a cylindrical column with an inner diameter of 8 cm and a height of 180 cm. The air and ozone gas were supplied from an air compressor and ozone generator systems, respectively. Sensitive gas-flow meters were employed in the apparatus to measure the gas-flow rate into the BCR. The bottom section of the BCR contained a gas distributor manufactured from stainless steel (i.e., perforated plate), with 52 holes that were 0.5 mm in size and were distributed in cycles in all of the plate areas.
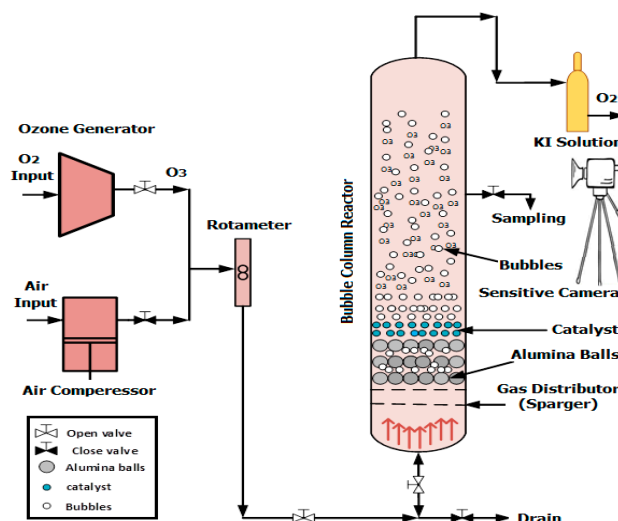

Figure 1. Schematic of the packed BCR when using alumina balls as the packing material.

Moreover, the photographs of the ozone gas bubbles were taken with a high-resolution and sensitive camera (Canon RF-S18), which was supplied with a professional video recorder. All images were taken in a specified zone at a height of 100 cm from the column bottom. The bubble images were processed and improved by utilizing Image Processing

MATLAB 9.10 Software (R2021a), which provides clear bubble sizes and bubble boundaries. Then, the size of the ozone gas bubbles was determined from image analysis. Furthermore, the uncertainty analysis measurement showed a standard error of deviation of ± 1.3 mm for the bubble size measurements.

2.3. Operating Procedure

In the present investigation, the ozonation reaction for phenol removal was achieved through using four treatment approaches in the BCR. The first approach was carried out in the BCR in the presence of ozone gas only. The second approach of phenol removal was achieved using alumina balls (α-Al$_2$O$_3$ of approximately zero surface area with no porosity) in the reactor with ozone gas, as shown in Figure 2. The diameter of each packing material was 20 mm, and they were supported in the BCR to a height of 0.7 m from the reactor bottom. Then, the void fraction between the packing materials inside the reactor was estimated to be 38%. The third treatment included the use of ZnO NPs as a nanocatalyst in the BCR with a dose of 0.05 g in the presence of ozone gas, while the fourth combined the packing material and ZnO nanocatalyst with ozone gas. Figure 3 summarizes the four operating approaches conducted in the BCR. Different concentrations of phenol in wastewater were used (i.e., 10, 15, 20, and 25 ppm). Dry air was fed to an ozone generator apparatus to produce high-purity ozone gas at a constant rate. The applied treatment time for the phenol material in the reactor was 10, 20, 30, 40, 50, 60, 70, 80, 90, and 100 min. The operating temperature and operating pressure were kept constant in the bubble column reactor at 25 °C and 1 bar, respectively, for all experiments. At the top of BCR, the output ozone gas was accumulated in a vertical collection vessel that was 1.5 L in size. This vessel contained a solution of potassium iodide (KI) with a concentration of 2%. The main purpose of this solution was to convert the unreacted ozone gas into oxygen according to the requirements of human safety and the environment.

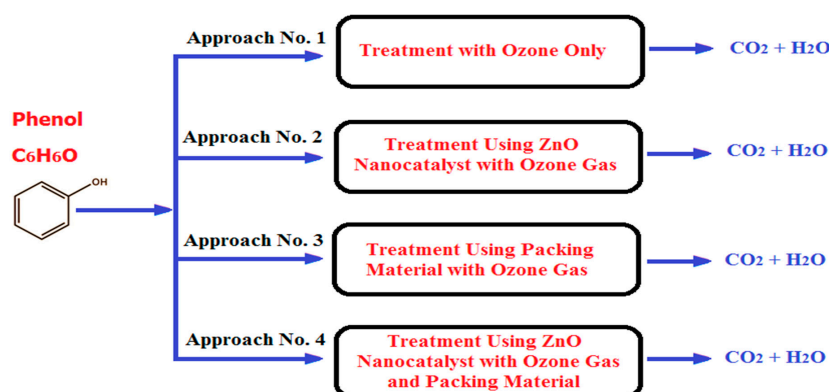**Figure 2.** Photograph of the alumina balls (α-Al$_2$O$_3$) packing material in the BCR.

Figure 3. The four experimental approaches conducted to remove phenol from the wastewater in the reaction system of a BCR.

Moreover, during each experiment, a sample from the reaction mixture was drawn from the sampling valve. The phenol concentration was measured using a total organic carbon (TOC) analyzer (E200, Shimadzu Co. Ltd., Kyoto, Japan). Further, many characterization devices were used to measure the main specifications of the ZnO nanocatalyst. The structural features were measured using a XRD-6000 Shimadzu, the morphology of nanoparticles was achieved using a FE-SEM (INSPECT F50-FEI, Philips, Eindhoven, The Netherlands), and the functional groups were evaluated using a FTIR device (IRTracer-100, Shimadzu, Kyoto, Japan). Also, the dispersion of the ZnO NPs was evaluated using a Zeta potential measuring device (Zeta Potential Analyzer, Zetasizer-ZEN3600, Malvern Panalytical Ltd., Malvern, UK).

3. Results and Discussion

3.1. Flow Behavior in the BCR

The hydrodynamic characterization of the BCR has an impact on its performance. It is well known from the literature that the flow regimes in the BCR are highly dependent on the gas velocity, pressure drop, gas holdup, and physical properties of the mixture [8,43,47]. Figure 4 shows the relationship between the superficial gas velocity and the gas holdup in the presence of ozone gas alone, as well as in the presence of ozone plus a ZnO nanocatalyst in the BCR. The majority of the flow at the applied gas velocity (less than 0.05 cm/s) was a homogeneous bubbly flow. Also, the bubble-size distribution was uniform, with a low bubble-rise velocity. The ozone gas superficial velocity was able to positively affect the BCR's performance. Additionally, it was found that the superficial gas velocity had a significant impact on the performance of the BCR due to its direct effect on the hydrodynamic parameters, such as gas holdup, bubble size, and rising velocity. Figure 4 shows that there was a slight variation in the gas holdup results in the BCR when using ozone with a ZnO nanocatalyst in comparison with using ozone gas alone. This variation was attributed to the change in the hydrodynamic behavior due to the presence of the ZnO nanocatalyst.
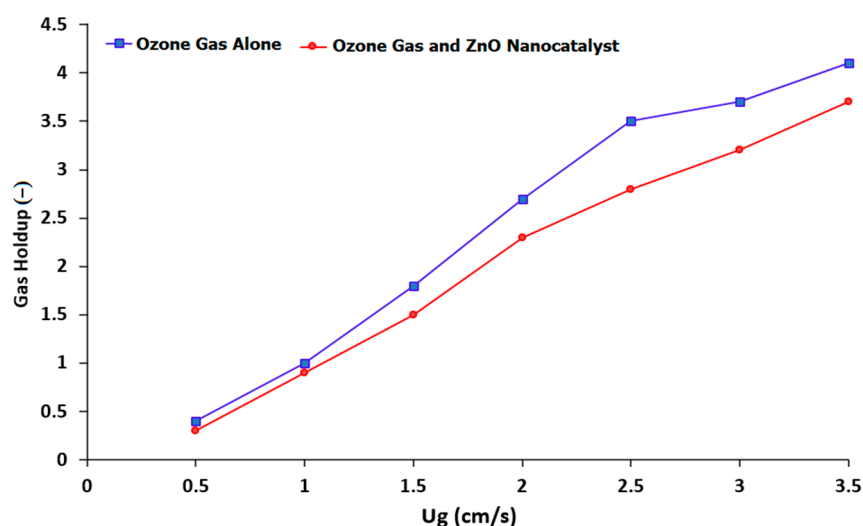

Figure 4. Influence of the superficial gas velocity on the gas holdup behavior in a BCR when using ozone alone and ozone gas in the presence of a ZnO nanocatalyst.

Figures 5 and 6 show the shapes of the gas bubbles in the BCR at various gas velocities when employing ozone gas alone and ozone gas with a ZnO nanocatalyst, respectively. Both figures demonstrate that, as the gas velocity rose, the bubble size increased as the small bubbles aggregated into large ones. Also, the general shape of the bubbles was spherical, with uniform distribution in the reactor at low gas velocities. Accordingly, at higher gas velocities (i.e., 3 cm/s), the bubble size grew and changed, forming ellipsoidal or slug shapes. This behavior can be explained by bubbles congregating and growing into larger bubbles. Numerous authors, including Sharma et al. [14], Barlak et al. [29], and

Alattar et al. [31], indicate that the gas velocity has a significant impact on the bubble size and shape in a BCR. A distinct increase in the gas holdup value in the reactor produces an increase in the effective interfacial area, which influences the mass-transfer process inside the reactor with the gas velocity.
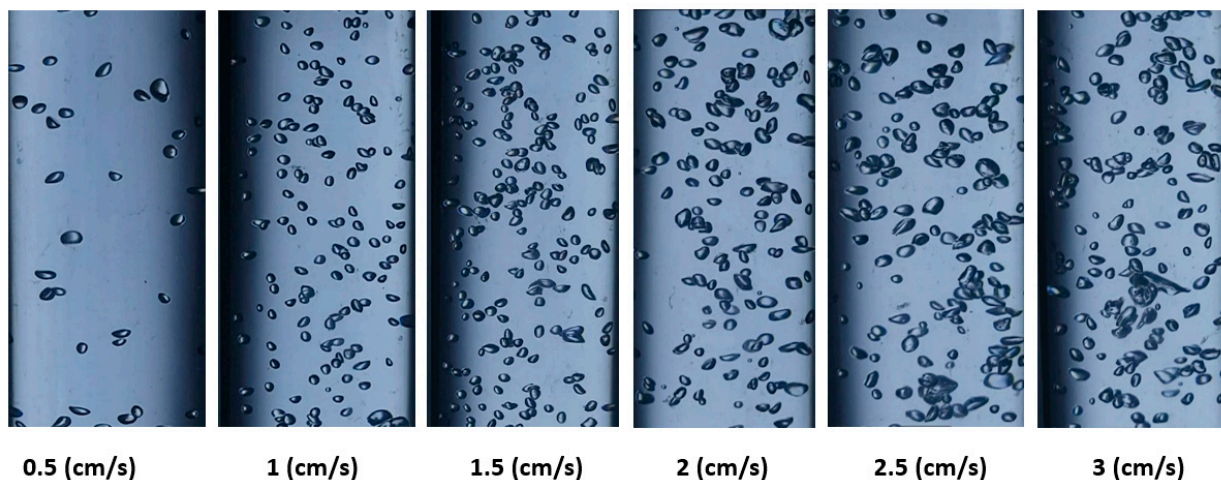

| 0.5 (cm/s) | 1 (cm/s) | 1.5 (cm/s) | 2 (cm/s) | 2.5 (cm/s) | 3 (cm/s) |

Figure 5. Variation in ozone bubbles at different superficial gas velocities in a BCR with ozone alone.

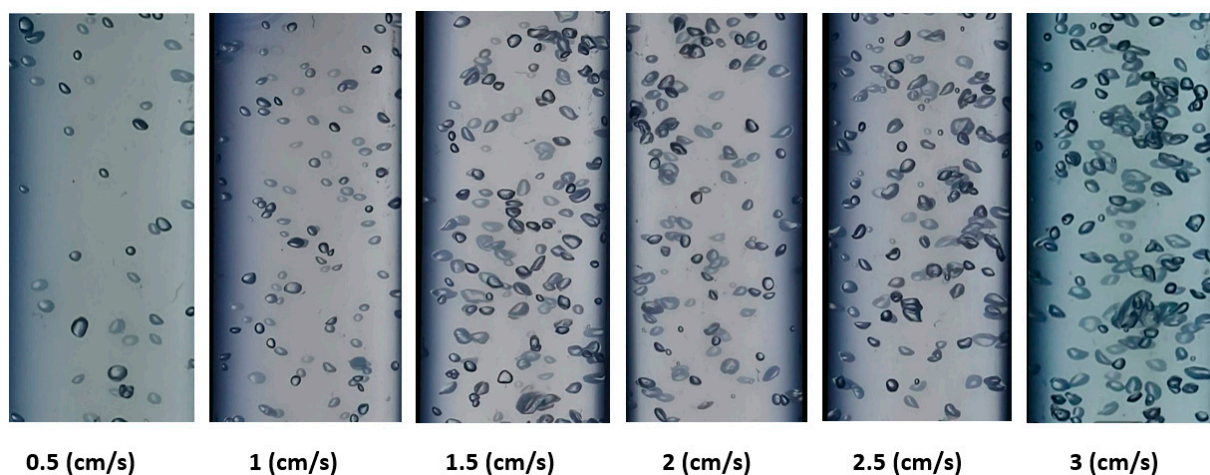| 0.5 (cm/s) | 1 (cm/s) | 1.5 (cm/s) | 2 (cm/s) | 2.5 (cm/s) | 3 (cm/s) |

Figure 6. Variation in ozone bubbles at different superficial gas velocities in a BCR with ozone gas plus a ZnO nanocatalyst.

The results of using ozone gas alone in the BCR can be seen in Figure 5, where the average bubble diameter was 0.44, 0.49, 0.55, 0.62, 0.68, and 0.72 cm at superficial gas velocities of 0.05, 1, 1.5, 2, 2.5, and 3 cm/s, respectively. Moreover, when using ozone with a ZnO nanocatalyst, the bubble size measured 0.48, 0.54, 0.58, 0.73, and 0.76 cm at the same aforementioned velocities, respectively. However, Figure 6 shows that the diameter of the bubbles increased more with the superficial gas velocity in the presence of the ZnO nanocatalyst in comparison with the case of the ozone gas alone. It was observed that the agglomeration processes caused the bubble diameter to grow along with the surface gas velocity, as also indicated by Lucas et al. [25]. The gas-bubble-formation mechanism in the BCR and their rising velocities mainly relate to the buoyancy phenomena that effectively influence the final hydrodynamic behavior in this type of reactor [8,31]. Usually, the rise of a bubble in the two-phase system in the dispersion appears due to coalescence and dispersion. Then, the bubbles can undergo a clear disengagement in the reactor. Malik et al. [36] and Jothinathan [46] pointed to the importance of bubble formation and bubble size in determining the effective reaction time between the gas and liquid phases. This phenomenon is the chief factor in determining the interfacial mixing in multiphase systems.

Therefore, in the present investigation, it was decided to use a superficial ozone gas velocity of 2.5 cm/s in all experiments due to their appropriate hydrodynamic characteristics for the reaction system in a BCR.

3.2. Characterization of the ZnO Nanocatalyst

The specifications of the ZnO nanocatalyst were characterized using various testing devices. The structural features of the nanocatalyst was characterized by an X-ray diffractometer to identify the main phases of the material structure. Figure 7 displays the X-ray diffraction pattern of the ZnO NPs. This figure clearly shows the presence of a number of peaks at 2θ, such as at 31.74, 34.42, 36.26, 47.57, 56.63, 62.89, 66.43, 67.95, 69.07, 72.69, and 76.86°, which corresponded to the Miller indices of the (100), (002), (101), (102), (110), (103), (200), (112), (201), (202), and (004) planes, respectively. Accordingly, it was found from the XRD results that a high crystalline structure of nano ZnO appeared with high purity.
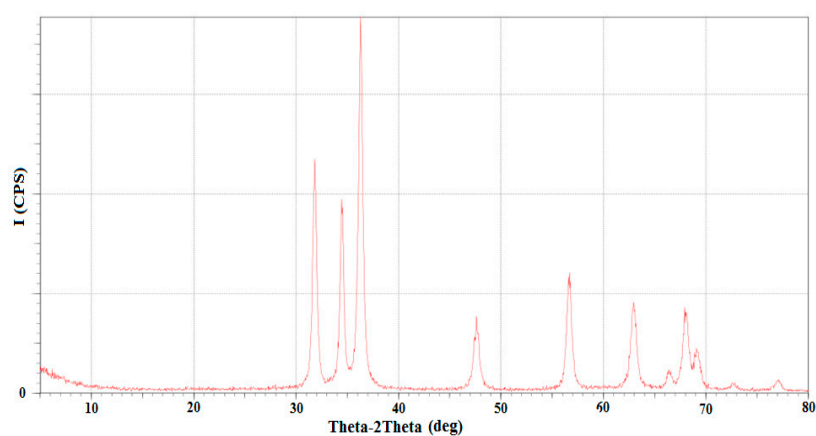

Figure 7. XRD analysis of the ZnO nanocatalyst.

Additionally, the morphological features of the ZnO nanocatalyst were measured using field emission scanning electron microscopy (FE-SEM). Figure 8 illustrates the FE-SEM results of the ZnO nanocatalyst at low and high magnifications, respectively. The general shape of the nanocatalyst was spherical, with a particle size of 28 nm. Such a small size is beneficial in dispersing the two-phase mixture in the BCR so as to provide an efficient distribution of the nanocatalyst within a sonication time of 15 min. Also, the FE-SEM results revealed that the ZnO NPs accumulated as clusters. To solve this problem, the ZnO nanocatalyst mixture was subjected to sonication in order to induce a high dispersion inside the BCR. Moreover, the Zeta potential measurements of the ZnO NPs had a Zeta potential value of −11.3 mV, which indicated a high stability and dispersion in the mixture for a long operating time in the reactor.
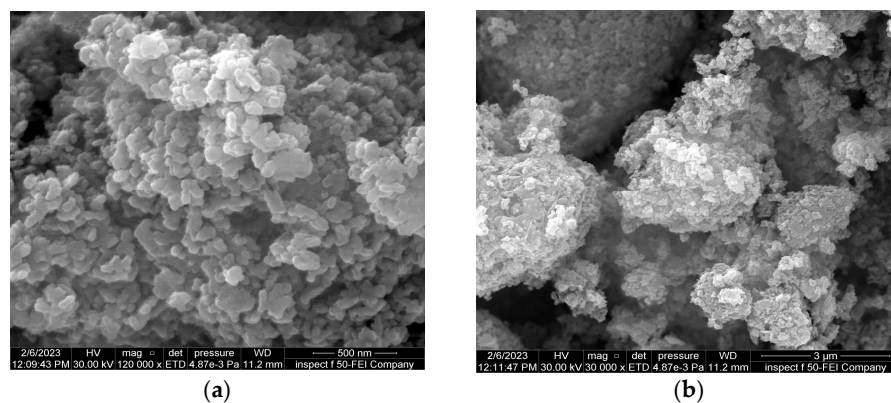

| (a) | (b) |

Figure 8. Morphological specifications of the ZnO NPs at (**a**) high and (**b**) low magnifications.

The functional groups associated with the ZnO nanocatalyst were identified using Fourier-transform infrared (FTIR) spectroscopy. Figure 9 shows the main vibrational bands of the ZnO nanocatalyst. The results indicated the presence of absorption bands at 3427.48, 2898.12, 1630.06, 1411.86, 1009.36, 907.63, and 663.61 cm^{-1}, which represent the main features of the ZnO. A summary of these bands and their positions follows. A clear absorption band was noted at 663.61 cm^{-1}, which is related to the metal–oxygen vibration (ZnO–stretching), while the band at 907.63 cm^{-1} corresponds to the vibration of the C–N or C–O bonds. Moreover, the bands at 1009.36 and 1411.86 cm^{-1} were related to the oxygen primary and secondary alcohol in-plane vibrations. The peak at 1630.06 cm^{-1} was ascribed to the aromatic nitro compounds and to alkyl vibration. In contrast, the bands at 2898.12 and 3427.48 cm^{-1} were ascribed to the stretching vibration of the hydroxyl compound.
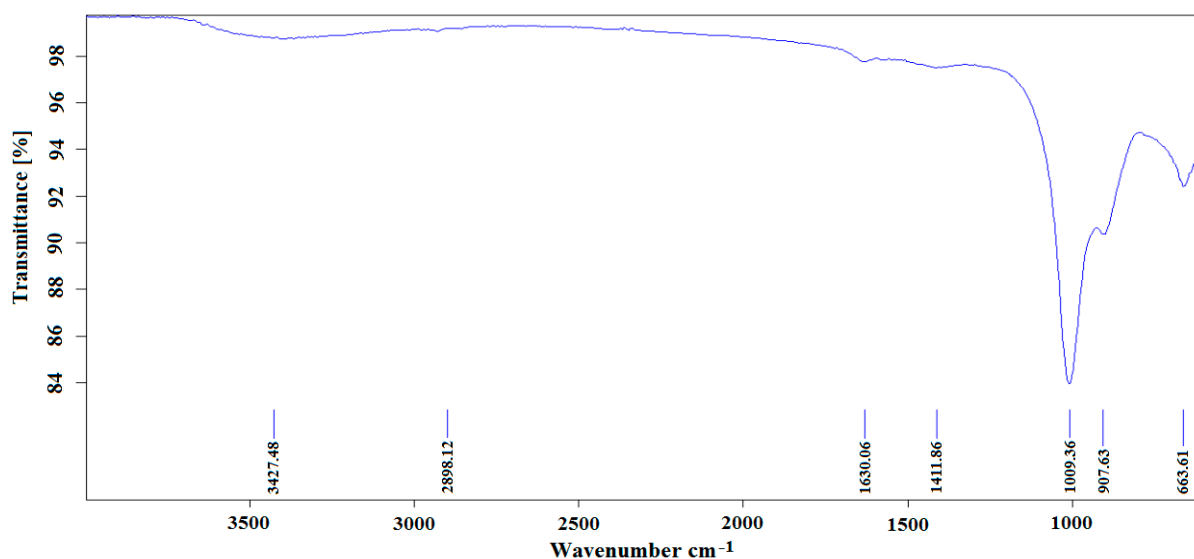

Figure 9. The main functional groups present in the ZnO nanocatalyst when using FTIR analysis.

3.3. Phenol Degradation Using Ozone Gas

The experiment was achieved using four phenol concentrations of 10, 15, 20, and 25 ppm. For all experimental runs, the pH value was held constant at 7, and the ozone rate was 3 g/h. The phenol degradation reaction was measured as a function of the treatment time in the BCR. Figure 10 illustrates the relationship between the reaction time and the percentage of phenol removal at various phenol concentrations. At phenol concentrations of 10, 15, 20, and 25 ppm, at a total reaction time of 50 min, the phenol removal was 65.82, 57.67, 53, and 43.64%, respectively. It was noted that, at the three phenol concentrations of 10, 15, and 20 ppm, the best reaction times were measured to be 80, 90, and 100 min, respectively. In addition, at an initial phenol concentration (low concentration) of 10 ppm, a reaction time of 100 min was necessary to provide an approximately 100% phenol removal. Additionally, as the initial phenol concentration increased, the duration of the reaction time also increased. As a result, the required reaction time was a function of the phenol concentration in the reactor, with this parameter being the main factor that determined the BCR performance. Lim et al. [1], Yamamoto et al. [15], and Zhou et al. [53] confirm the importance of the reaction time in phenol degradation.
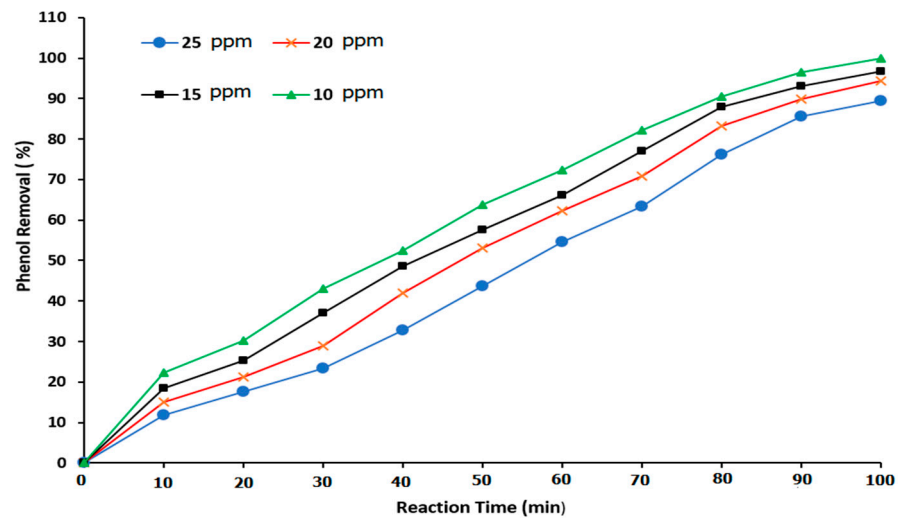
Figure 10. Effect of the reaction time on the phenol degradation when using ozone gas alone.

3.4. Phenol Degradation Using Ozone Gas and a ZnO Nanocatalyst

According to the results of Cheng et al. [2] and Ratman et al. [11], the ozonation reaction was slightly low due to a low mass-transfer operation. Therefore, more reaction time was required to achieve efficient phenol degradation. As such, the use of heterogeneous catalysts can activate the reaction mechanism of phenol degradation and enhance the ozonation process in the BCR. Accordingly, ZnO NPs were used as the nanocatalyst in the reaction system. Figure 11 illustrates the influence of the addition of 0.05 g of the ZnO nanocatalyst in the BCR on the phenol removal in relation to the reaction time. The results showed a clear enhancement in the phenol degradation reaction due to the presence of the ZnO nanocatalyst in comparison with the results of using ozone gas alone (Figure 10). Moreover, at a reaction time of 50 min, the phenol removal values were 73.63, 64.921, 56.697, and 49.7% at phenol concentrations of 10, 15, 20, and 25 ppm, respectively. It was found that the ZnO nanocatalyst worked by initiating the ozonation process so as to degrade the phenol from wastewater at a high rate. This process exhibited great potential in treating complex hydrocarbons efficiently. The presence of a ZnO nanocatalyst positively affects three factors: (1) the active removal of phenol, (2) lowering the amount of consumed treatment energy, and (3) the economic cost [17,38,54].
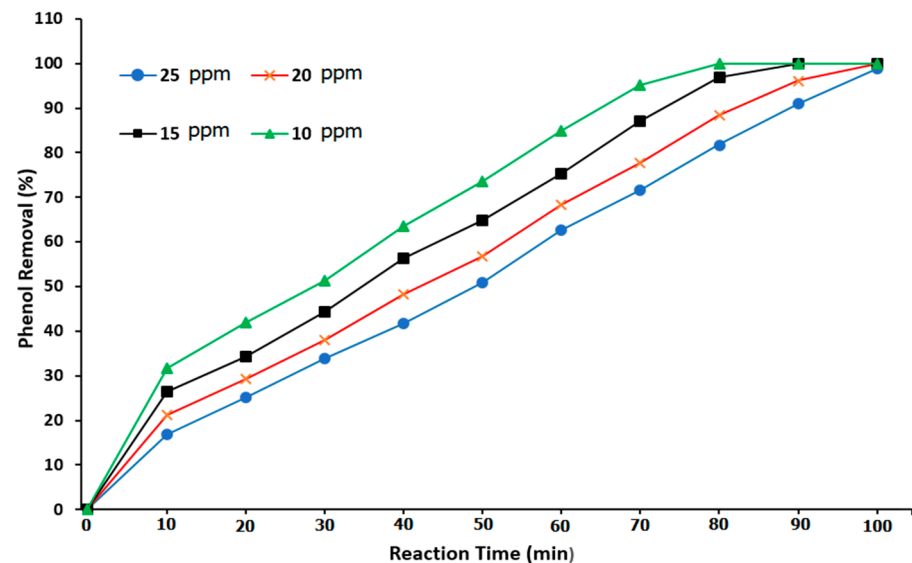

Figure 11. Effect of the reaction time on the phenol degradation when using ozone and a ZnO nanocatalyst in a BCR.

Furthermore, to achieve the complete degradation of phenol, Figure 10 shows that the reaction times of 80, 90, and 100 min were required at phenol concentrations of 10, 15, and 20 ppm, respectively. However, when using ozone alone without the ZnO nanocatalyst, the required reaction times were longer for the complete removal of phenol. In that case, a reaction time of 100 min was required to remove 10 ppm of phenol. The use of the ZnO nanocatalyst provided a high surface area and thus increased the reaction rate within a short reaction time. The increase in the conversion of phenol during the catalyst's ozonation process was mostly due to the effect of the free radicals produced by the self-decomposition of ozone on the active site of the ZnO nanocatalyst [31,42].

3.5. Phenol Degradation Using Ozone and α-Al₂O₃ as a Packing Material in a BCR

The low solubility of ozone gas in water remains one of the main challenges in the ozonation reaction. Accordingly, a long reaction time is usually required to overcome this problem. Thus, the use of high-surface-area packing material in the BCR can greatly increase the mass-transfer and reaction rate. Figure 12 shows the relationship between phenol removal and reaction time in the BCR when using ozone and $\alpha\text{-}Al_2O_3$ as a packing material. The degradation rate of phenol removal increased at a low applied phenol concentration. For phenol concentrations of 10, 15, 20, and 25 ppm, the percentage of phenol removal was 77.63, 71.4, 63.99, and 56.38%, respectively. Also, the use of a packing material in the BCR provided a removal of 100% for the phenol concentrations of 10, 15, and 20 ppm at reaction times of 80, 90, and 100 min, respectively. Such results contribute to a clear picture of the influence of alumina balls as packing material on the ozonation reaction in a BCR.
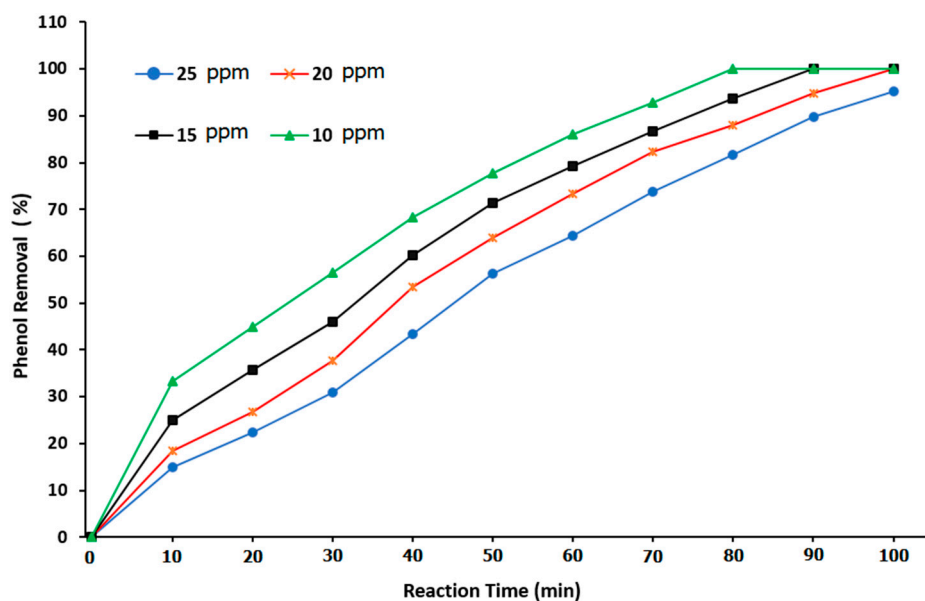

Figure 12. Effect of the reaction time on the phenol degradation when using ozone and Al_2O_3 as a packing material in a BCR.

On the other hand, the potassium iodide (KI) of the ozone-gas evaluation test demonstrated that the packing had a positive impact on the mass-transfer coefficient and contact time. The KI test showed a concentration of 3.5 ppm for the produced ozone without packing, but only 0.20 ppm in the presence of packing. Figure 13 explains the change in the appearance of the KI solution, which indicated a higher ozone concentration when packing material was used. Also, this appearance of the KI solution signified the high mass-transfer efficiency due to an available high total surface area for the ozonation reaction with packing material.
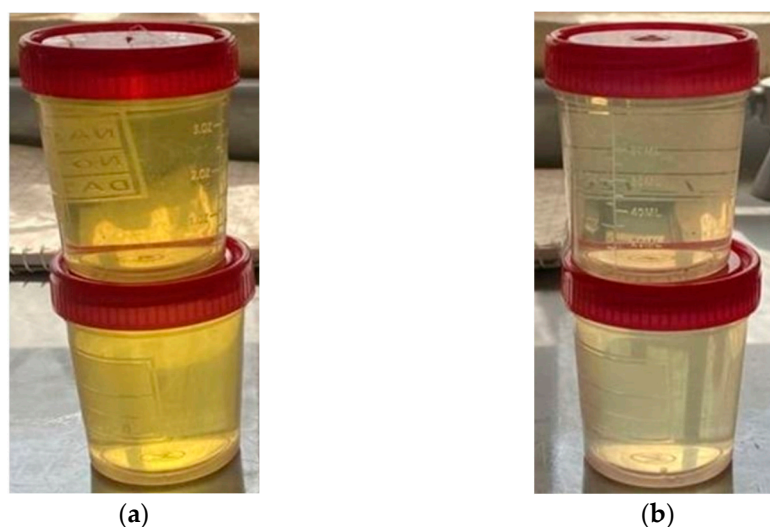
<table>
<tr><td>(a)</td><td>(b)</td></tr>
</table>

Figure 13. Change in the appearance of the potassium iodide (KI) solution (**a**) without packing and (**b**) in the presence of packing.

The presence of packing material provided a higher mass-transfer performance [18,40]. However, the pressure drops in the BCR that were expected to appear did not, and this was due to the large particle size of the α-Al$_2$O$_3$ packing material, which showed a high void fraction (45%) in the reactor. Accordingly, the expected beneficial influence of the pressure drop on the reactor performance was limited. The use of commercial α-Al$_2$O$_3$ packing in the reactor increased the contact surface area between the gas and liquid phases. Fortunately, the enhancement in the mass-transfer process made up for the small pressure drop; therefore, the overall mechanism improved the ozonation reaction of phenol. Additionally, a thin film usually formed over the surface of the packing material, and this played a constant role in enhancing the mass-transfer mechanism by improving the liquid distribution, wettability, and—ultimately—the reaction rate in the BCR. This aspect is critical in chemical reactions because of the limited reaction rate of the ozonation process. The diffusion mechanism across the thin film provided a clear improvement in the degradation of phenol in wastewater. Moreover, the BCR as a multiphase reactor is usually characterized by efficient mass and heat transfer due to the high efficiency of the hydrodynamic parameters [8,14]. As shown in Section 3.1, in the present experimental study, the hydrodynamic parameters were evaluated and managed to provide an optimal performance in the BCR.

3.6. Phenol Degradation When Using Ozone, α-Al$_2$O$_3$ packing, and a ZnO Nanocatalyst

The fourth experiment included phenol treatment with ozone gas by utilizing a ZnO nanocatalyst in the presence of α-Al$_2$O$_3$ packing, as shown in Figure 14. For a phenol concentration of 10 ppm, a conversion rate of 100% was achieved with respect to the phenol elimination in the reactor at a reaction time of 70 min with a 0.05 g ZnO nanocatalyst. Accordingly, at phenol concentrations of 15, 20, and 25 ppm, the phenol removal measurements showed values of 94, 89.213, and 80.85%, respectively. Also, the results indicated that the phenol concentrations of 25, 20, and 15 ppm required reaction times of 100, 90, and 80 min, respectively, to achieve the complete (100%) degradation of phenol. The development in phenol removal resulted from the hydrodynamic characteristics in the BCR, including the increased interfacial area, low ozone bubble rising velocity, extended gas stagnation time, increased reaction time, and a high mass-transfer process. All of these parameters reflect the high efficiency of the phenol conversion rate. The presence of the packing material and the ZnO nanocatalyst improved the mechanism of the ozonation reaction so as to provide a high-performance effect in the BCR. These results agree with the results of Li et al. [7], Gao et al. [38], and Wei et al. [43].
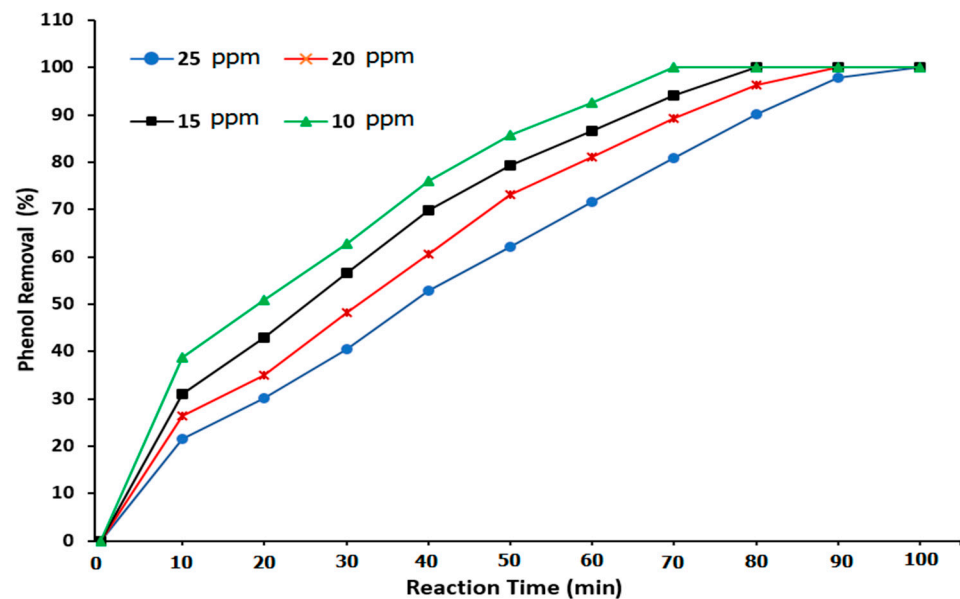
Figure 14. Effect of the reaction time on the phenol degradation when using ozone, packing material, and a ZnO nanocatalyst in a BCR.

Figure 15 illustrates the comparison between the four experimental approaches of phenol removal when using ozone alone, ozone with a packing material, ozone with a ZnO nano-catalyst, and ozone with packing material + a ZnO nanocatalyst (at 10 ppm of phenol concentration). From this figure, it was noted that the phenol removal efficiency recorded the highest value of 100% at 70 min of reaction time by employing the experimental approach that used ozone gas in the presence of both α-Al$_2$O$_3$ packing and a ZnO nanocatalyst. In actuality, in this combined approach, the ozonation reaction rate was enhanced due to the high contact surface area between the gas and liquid phase. Then, a clear chance was achieved in terms of low gas holdup and an effective interfacial area so as to provide appropriate reaction conditions for a 100% phenol degradation with a shorter reaction time. The same observation was noted by Guo et al. [19] and Alattar et al. [31].
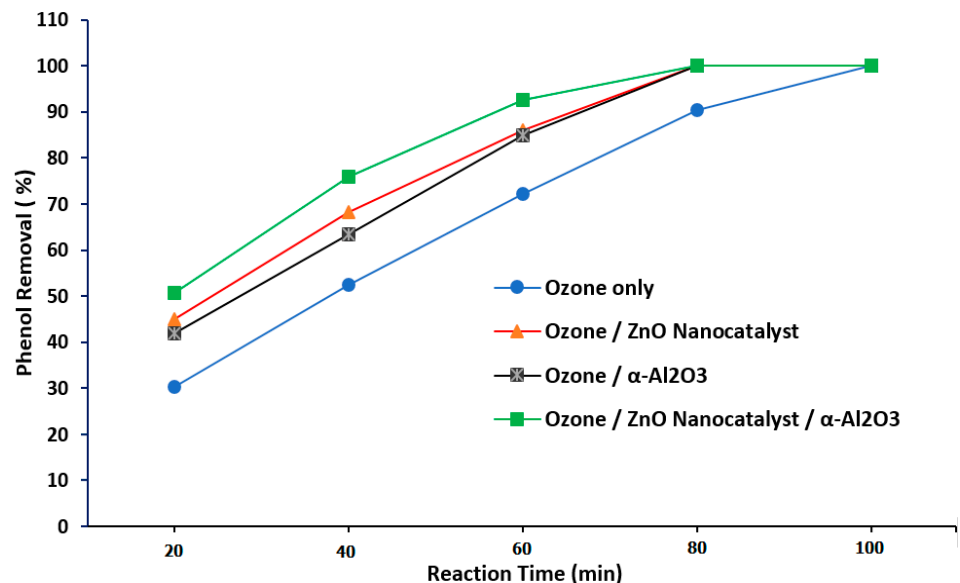

Figure 15. Comparison of the results of phenol degradation when using the four experimental modes of ozone alone, ozone with packing material, ozone with a ZnO nanocatalyst, and ozone with packing material + a ZnO nanocatalyst (at 10 ppm of phenol concentration).

3.7. Reaction Kinetics of the Process

In order to provide a clear understanding of the phenol reaction in the ozonation process in a BCR, a kinetics study was conducted. Accordingly, a first-order reaction was assumed depending on the phenol concentrations and reaction time, as shown in Figure 16. Moreover, the four experimental approaches of ozone alone (A), ozone with a ZnO nanocatalyst (B), ozone with packing material (C), and ozone with both packing material + a ZnO nanocatalyst (D) were evaluated. Therefore, the main mathematical equation for the first-order assumption is shown in Equation (1):

$$\text{Ln}[C_A/C_{Ao}] = -k_1\, t \tag{1}$$

where C_{Ao} is the initial concentration of phenol in (mg/l) at a reaction time = 0, C_A represents the concentration of phenol in (mg/l) at any time (t), and k_1 is the reaction rate constant for the first-order (1/min).
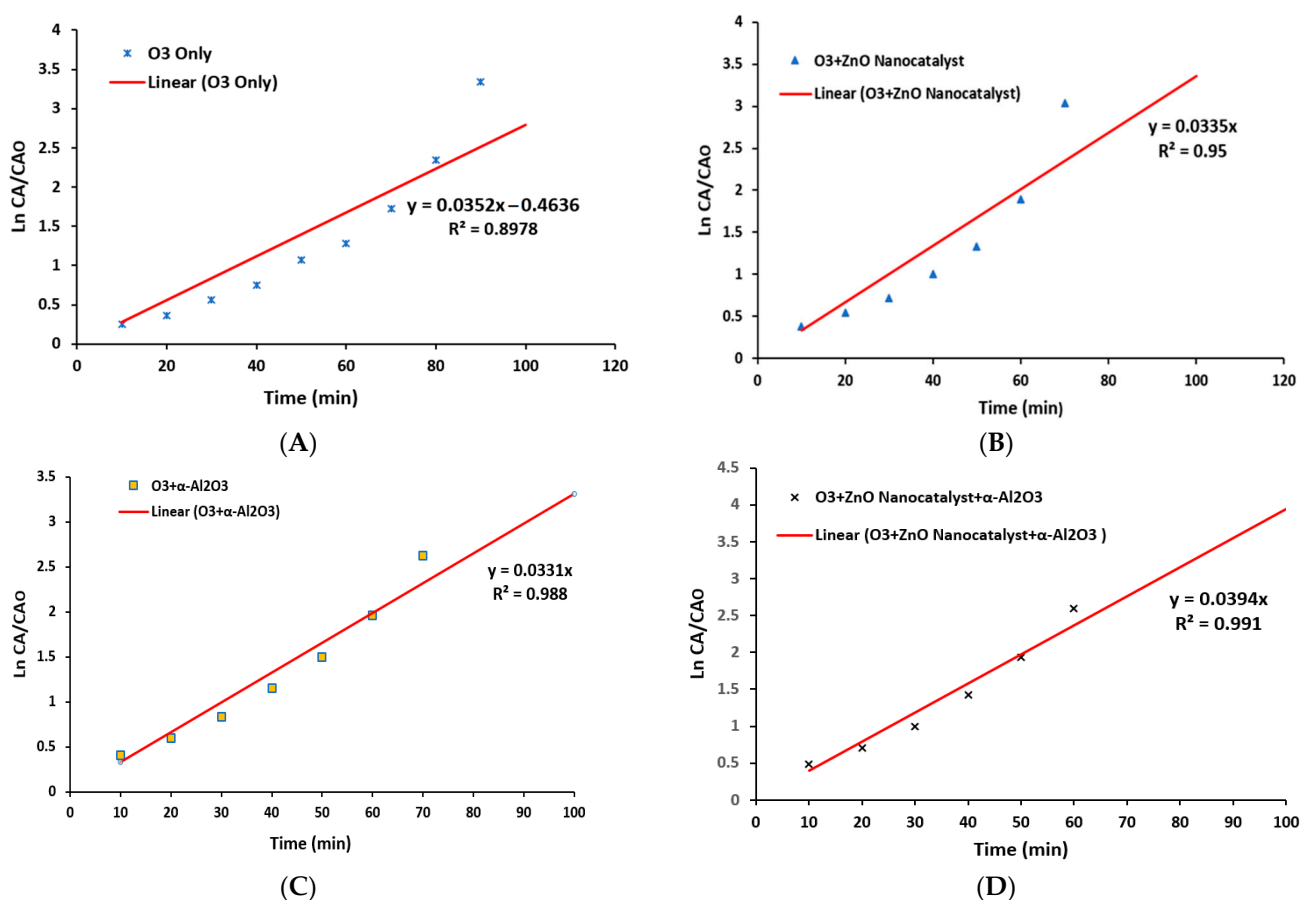

Figure 16. The results of the kinetics study in a first-order assumption for phenol degradation reaction via an ozonation process conducted with four experimental approaches: (**A**) ozone alone, (**B**) ozone with a ZnO nanocatalyst, (**C**) ozone with packing material, and (**D**) ozone with both packing material + a ZnO nanocatalyst.

The operating conditions were 3 g/h of ozone dosage, 10 mg/L of phenol, and 0.05 g/L of the ZnO nanocatalyst in the presence of α-AL$_2$O$_3$ as the packing material. Figure 16 shows the relationship between $\text{Ln}[C_A/C_{Ao}]$ and the reaction time. Then, the slope (k_1) can be determined from this figure as the best-fit line. Figure 16A–D showed that the correlation coefficient (R^2) recorded high values of 0.897, 0.95, 0.988, and 0.991, respectively. Accordingly, the results of the theoretical and practical evaluation indicated that the reaction kinetics results of a first-order assumption was in high accordance with the real reaction behavior of the phenol degradation. Furthermore, from the results of

Figure 16, it is clear that the experimental approach of an ozonized packed BCR with a ZnO nanocatalyst (case D) showed the highest value of an R^2 of 0.991 with a reaction rate constant of k_1 = 0.1683 1/min. The determination of the reaction order is the key factor toward understanding the relationship between the rate of reaction and the concentrations of reactants inside the reactor.

From a reaction kinetics point of view, the presence of nanocatalysts in the ozonation process promote the decomposition of ozone gas into hydroxyl radicals [17,34]. Sable et al. [40] and Honarmandrad et al. [45] have shown that the catalytic ozonation reaction is a modified oxidation process, which includes the formation of highly active free radicals that initiate the degradation of organic pollutants at a high rate. Therefore, the present investigation showed a high level of phenol degradation due to the combination of a $\alpha\text{-}Al_2O_3$ packing material and a ZnO nano-catalyst in the reaction system. The addition of a ZnO nanocatalyst to wastewater containing phenol provided a clear increase in the gas holdup and reaction surface area, as well as a high dispersion of the nanocatalyst particles. All of these factors promoted the consumption of a high quantity of ozone in the reaction mixture, causing the phenol degradation process to improve significantly by forming water and carbon dioxide. Accordingly, a shorter reaction time was required for phenol degradation when applying this method, and this produced a high-performance removal in a BCR [4,24,50].

4. Conclusions

In this study, the problem of a limited ozonation reaction rate was solved in a bubble column reactor (BCR). The ozonation reaction of the phenol degradation was improved in a BCR by utilizing $\alpha\text{-}Al_2O_3$ as a packing material and a ZnO nanocatalyst. The results indicated that the presence of packing is suitable for a high mass-transfer mechanism due to the high total contact surface area between the gas and liquid phases. Also, the high void fraction of the packing material (45%) maintained the pressure drop inside the reactor within an acceptable limit without influencing the reaction rate. Moreover, it was found that the ZnO nanocatalyst improved the phenol degradation rate dramatically by enhancing the phenol degradation mechanism. The experimental results showed that as the phenol concentration increased in the reaction system, it required additional time for the ozonation reaction. Also, the presence of $\alpha\text{-}Al_2O_3$ balls and the ZnO nanocatalyst showed the highest phenol removal values. Further, it was observed that the hydrodynamic parameters of the BCR played a major role in determining the BCR's performance in the reaction process. A phenol concentration of 25, 20, and 15 ppm required a reaction time of 100, 90, and 80 min, respectively, to achieve the complete (100%) degradation of the phenol. Additionally, the understanding of the ozonation reaction mechanisms achieved in this work was necessary in order to apply this method in wastewater system treatment at industrial plants.

References

1. Lim, S.; Shi, J.L.; von Gunten, U.; McCurry, D.L. Ozonation of organic compounds in water and wastewater: A critical review. *Water Res.* **2022**, *213*, 118053. [CrossRef] [PubMed]

2. Cheng, W.; Quan, X.; Li, R.; Wu, J.; Zhao, Q. Ozonation of phenol-containing wastewater using $O_3/Ca(OH)_2$ system in a microbubble gas-liquid reactor. *Ozone Sci. Eng.* **2018**, *40*, 173–182. [CrossRef]

3. Miao, F.; Zhang, S.; Sun, X.; Li, Y.; Shang, R.; Wu, W.; Jiao, W.; Liu, Y. Degradation of phenol with $Mn-CoO_X/\gamma-Al_2O_3$ catalytic ozonation enhanced by high gravity technology. *Chem. Eng. Sci.* **2023**, *280*, 119036. [CrossRef]

4. Derco, J.; Gotvajn, A.Ž.; Čižmárová, O.; Dudáš, J.; Sumegová, L.; Šimovičová, K. Removal of micropollutants by ozone-based processes. *Processes* **2021**, *9*, 1013. [CrossRef]

5. Mohamadi, L.; Bazrafshan, E.; Rahdar, A.; Labuto, G.; Kamali, A.R. Nanostructured MgO-enhanced catalytic ozonation of petrochemical wastewater. *Bol. Soc. Esp. Cerám. Vidr.* **2021**, *60*, 391–400. [CrossRef]

6. Zhang, F.; Wei, C.; Hu, Y.; Wu, H. Zinc ferrite catalysts for ozonation of aqueous organic contaminants: Phenol and bio-treated coking wastewater. *Sep. Purif. Technol.* **2015**, *156*, 625–635. [CrossRef]

7. Li, X.; Fu, L.; Chen, F.; Zhao, S.; Zhu, J.; Yin, C. Application of heterogeneous catalytic ozonation in wastewater treatment: An overview. *Catalysts* **2023**, *13*, 342. [CrossRef]

8. Lima, V.N.; Rodrigues, C.S.; Sampaio, E.F.; Madeira, L.M. Insights into real industrial wastewater treatment by Fenton's oxidation in gas-bubbling reactors. *J. Environ. Manag.* **2020**, *265*, 110501. [CrossRef]

9. Wu, T.; Zhang, H.; Liu, Z.; Liu, T.; Jiang, P.; Arowo, M.; Shao, L. Amaranth wastewater treatment by intensified ozonation in a rotating zigzag bed. *J. Water Process Eng.* **2022**, *49*, 102984. [CrossRef]

10. Van Aken, P.; Van den Broeck, R.; Degrève, J.; Dewil, R. A pilot-scale coupling of ozonation and biodegradation of 2, 4-dichlorophenol-containing wastewater: The effect of biomass acclimation towards chlorophenol and intermediate ozonation products. *J. Clean. Prod.* **2017**, *161*, 1432–1441. [CrossRef]

11. Ratman, I.; Kusworo, T.D.; Utomo, D.P.; Azizah, D.A.; Ayodyasena, W.A. Petroleum refinery wastewater treatment using three steps modified nanohybrid membrane coupled with ozonation as integrated pre-treatment. *J. Environ. Chem. Eng.* **2020**, *8*, 103978. [CrossRef]

12. Mousa, N.E.; Mohammed, S.S.; Shnain, Z.Y.; Abid, M.F.; Alwasiti, A.A.; Sukkar, K.A. Catalytic photodegradation of cyclic sulfur compounds in a model fuel using a bench-scale falling-film reactor irradiated by a visible light. *Bull. Chem. React. Eng. Catal.* **2022**, *17*, 755–767. [CrossRef]

13. Muddemann, T.; Neuber, R.; Haupt, D.; Graßl, T.; Issa, M.; Bienen, F.; Enstrup, M.; Möller, J.; Matthée, T.; Sievers, M.; et al. Improving the treatment efficiency and lowering the operating costs of electrochemical advanced oxidation processes. *Processes* **2021**, *9*, 1482. [CrossRef]

14. Sharma, S.; Chokshi, N.; Ruparelia, J.P. Effect of operating parameters on O_3, O_3/UV, $O_3/UV/PS$ process using bubble column reactor for degradation of reactive dyes. *J. Inst. Eng. (India) Series A* **2023**, *104*, 565–578. [CrossRef]

15. Yamamoto, T.; Iimura, K.; Satone, H.; Itoh, K.; Maeda, K. Ozonation of aqueous phenol using high-silica zeolite in an aerated mixing vessel. *Asia-Pac. J. Chem. Eng.* **2018**, *13*, e2175. [CrossRef]

16. Shanian, Z.Y.; Abid, M.F.; Sukkar, K.A. Photodegradation of mefenamic acid from wastewater in a continuous flow solar falling film reactor. *Desalination Water Treat.* **2021**, *210*, 22–30. [CrossRef]

17. Nedeltchev, S. Unified approach for prediction of the volumetric mass transfer coefficients in a homogeneous and heterogeneous bubble column based on the non-corrected penetration theory: Case studies. *Processes* **2022**, *10*, 1828. [CrossRef]

18. Flagiello, D.; Tammaro, D.; Erto, A.; Maffettone, P.L.; Lancia, A.; Di Natale, F. Foamed structured packing for mass-transfer equipment produced by an innovative 3D printing technology. *Chem. Eng. Sci.* **2022**, *260*, 117853. [CrossRef]

19. Guo, H.; Li, X.; Li, G.; Liu, Y.; Rao, P. Preparation of $SnO_x-MnOx@ Al_2O_3$ for catalytic ozonation of phenol in hypersaline wastewater. *Ozone Sci. Eng.* **2023**, *45*, 262–275. [CrossRef]

20. Mohammed, A.A.; Sukkar, K.A.; Shnain, Z.Y. Effect of graphene and multiwalled carbon nanotube additives on the properties of nano-reinforced rubber. *Chem. Pap.* **2021**, *75*, 3265–3272. [CrossRef]

21. Van Aken, P.; Van den Broeck, R.; Degrève, J.; Dewil, R. The effect of ozonation on the toxicity and biodegradability of 2, 4-dichlorophenol-containing wastewater. *Chem. Eng. J.* **2015**, *280*, 728–736. [CrossRef]

22. Zhang, S.; Zhou, L.; Li, Z.; Esmailpour, A.A.; Li, K.; Wang, S.; Liu, R.; Li, X.; Yun, J. Efficient treatment of phenol wastewater by catalytic ozonation over micron-sized hollow MgO rods. *ACS Omega* **2021**, *6*, 25506–25517. [CrossRef] [PubMed]

23. Pokkiladathu, H.; Farissi, S.; Muthukumar, A.; Muthuchamy, M. Removal of a contaminant of emerging concern by heterogeneous catalytic ozonation process with a novel nano bimetallic catalyst embedded on activated carbon. *Ozone Sci. Eng.* **2022**, *45*, 361–373. [CrossRef]

24. Almukhtar, R.; Hammoodi, S.I.; Majdi, H.S.; Sukkar, K.A. Managing transport processes in thermal cracking to produce high-quality fuel from extra-heavy waste crude oil using a semi-batch reactor. *Processes* **2022**, *10*, 2077. [CrossRef]

25. Lucas, M.S.; Peres, J.A.; Lan, B.Y.; Puma, G.L. Ozonation kinetics of winery wastewater in a pilot-scale bubble column reactor. *Water Res.* **2009**, *43*, 1523–1532. [CrossRef]

26. Li, X.; Chen, W.; Ma, L.; Wang, H.; Fan, J. Industrial wastewater advanced treatment via catalytic ozonation with an Fe-based catalyst. *Chemosphere* **2018**, *195*, 336–343. [CrossRef]

27. Jasim, M.A.; AlJaberi, F.Y. Removal of COD from real oily wastewater by electrocoagulation using a new configuration of electrodes. *Environ. Monitor. Assess.* **2023**, *195*, 1–17. [CrossRef]

28. Ajeel, S.A.; Sukkar, K.A.; Zedin, N.K. New magnesia-thermal reduction technique to produce high-purity crystalline nano-silicon via semi-batch reactor. *Mater. Today Proc.* **2021**, *42*, 1966–1972. [CrossRef]

29. Barlak, M.S.; Değermenci, N.; Cengiz, I.; Özel, H.U.; Yildiz, E. Comparison of phenol removal with ozonation in jet loop reactor and bubble column. *J. Environ. Chem. Eng.* **2020**, *8*, 104402. [CrossRef]

30. Jin, X.; Wu, C.; Fu, L.; Tian, X.; Wang, P.; Zhou, Y.; Zuo, J. Development, dilemma and potential strategies for the application of nanocatalysts in wastewater catalytic ozonation: A review. *J. Environ. Sci.* **2023**, *124*, 330–349. [CrossRef]

31. Alattar, S.A.; Sukkar, K.A.; Alsaffar, M.A. The role of TiO_2 NPs catalyst and packing material in removal of phenol from wastewater using an ozonized bubble column reactor. *Acta Innov.* **2023**, *46*, 90–101. [CrossRef]

32. Yan, P.; Ye, Y.; Wang, M. Catalytic ozonation of phenol by $ZnFe_2O_4$/ZnNCN: Performance and mechanism. *Environ. Sci. Pollut. Res.* **2022**, *29*, 88172–88181. [CrossRef] [PubMed]

33. Awad, A.M.; Sukkar, K.A.; Jaed, D.M. Development of an extremely efficient Iraqi nano-lubricating oil (Base-60) employing SiO_2 and Al_2O_3 nanoparticles. *AIP Conf. Proc.* **2022**, *2443*, 1.

34. Xiao, J.; Xie, Y.; Cao, H. Organic pollutants removal in wastewater by heterogeneous photocatalytic ozonation. *Chemosphere* **2015**, *121*, 1–17. [CrossRef]

35. Wang, J.; Yuan, S.; Dai, X.; Dong, B. Application, mechanism, and prospects of Fe-based/Fe-biochar catalysts in heterogenous ozonation process: A review. *Chemosphere* **2023**, *319*, 138018. [CrossRef]

36. Malik, S.N.; Ghosh, P.C.; Vaidya, A.N.; Mudliar, S.N. Hybrid ozonation process for industrial wastewater treatment: Principles and applications: A review. *J. Water Process Eng.* **2020**, *35*, 101193. [CrossRef]

37. Baqur, M.S.; Hamied, R.S.; Sukkar, K.A. An eco-friendly process to produce high-purity nano-γ-Al_2O_3 from aluminum scrap using a novel electrolysis technique for petroleum industry applications. *Arabian J. Sci. Eng.* **2023**, 1–11. [CrossRef]

38. Gao, K.; Shao, S.; Li, Z.; Jing, J.; Jiao, W.; Liu, Y. Kinetics of the direct reaction between ozone and phenol by high-gravity intensified heterogeneous catalytic ozonation. *Chin. J. Chem. Eng.* **2023**, *53*, 317–323. [CrossRef]

39. Saputera, W.H.; Putrie, A.S.; Esmailpour, A.A.; Sasongko, D.; Suendo, V.; Mukti, R.R. Technology advances in phenol removals: Current progress and future perspectives. *Catalysts* **2021**, *11*, 998. [CrossRef]

40. Sable, S.S.; Shah, K.J.; Chiang, P.C.; Lo, S.L. Catalytic oxidative degradation of phenol using iron oxide promoted sulfonated-ZrO_2 by advanced oxidation processes (AOPs). *J. Taiwan Inst. Chem. Eng.* **2018**, *91*, 434–440. [CrossRef]

41. Hamied, R.S.; Ali, A.N.M.; Sukkar, K.A. Enhancing heavy crude oil flow in pipelines through heating-induced viscosity reduction in the petroleum industry. *Fluid Dyn. Mater. Process.* **2023**, *19*. [CrossRef]

42. Ghaisani, S.V.; Wahyudi, D.P.; Enjarlis, E.; Karamah, E.F.; Bismo, S. Performance of phenolic wastewater degradation with ozonation and catalytic ozonation technique in multi-injection bubble column reactor. *AIP Conf. Proc.* **2019**, *2175*, 1.

43. Wei, X.; Shao, S.; Ding, X.; Jiao, W.; Liu, Y. Degradation of phenol with heterogeneous catalytic ozonation enhanced by high gravity technology. *J. Clean. Prod.* **2020**, *248*, 119179. [CrossRef]

44. Rahman–Al Ezzi, A.A. Phenol removal using pulsation bubble column with inverse fluidization airlift loop reactor. *Chem. Ind. Chem. Eng. Q.* **2021**, *27*, 99–106. [CrossRef]

45. Honarmandrad, Z.; Javid, N.; Malakootian, M. Removal efficiency of phenol by ozonation process with calcium peroxide from aqueous solutions. *Appl. Water Sci.* **2021**, *11*, 14. [CrossRef]

46. Jothinathan, L.; Cai, Q.Q.; Ong, S.L.; Hu, J.Y. Organics removal in high strength petrochemical wastewater with combined microbubble-catalytic ozonation process. *Chemosphere* **2021**, *263*, 127980. [CrossRef]

47. Alattar, S.A.; Sukkar, K.A.; Alsaffar, M.A. Enhancement of ozonation reaction for efficient removal of phenol from wastewater using a packed bubble column reactor. *Indones. J. Chem.* **2023**, *23*, 383–394. [CrossRef]

48. Bhosale, G.S.; Vaidya, P.D.; Joshi, J.B.; Patil, R.N. Analysis of reaction kinetics of the ozonation of phenolic compounds and assessment of the role of mass transfer in the overall rate. *Ind. Eng. Chem. Res.* **2023**, *62*, 8181–8190. [CrossRef]

49. Ferreiro, C.; de Luis, A.; Villota, N.; Lomas, J.M.; Lombraña, J.I.; Camarero, L.M. Application of a Combined Adsorption−Ozonation Process for Phenolic Wastewater Treatment in a Continuous Fixed-Bed Reactor. *Catalysts* **2021**, *11*, 1014. [CrossRef]

50. Javed, S.; Mirza, C.R.; Khan, A.H.A.; Khalifa, W.; Achour, B.; Barros, R.; Yousaf, S.; Butt, T.A.; Iqbal, M. Limited phosphorous supply improved lipid content of Chlorella vulgaris that increased phenol and 2-chlorophenol adsorption from contaminated water with acid treatment. *Processes* **2022**, *10*, 2435. [CrossRef]

51. Chen, C.; Yoza, B.A.; Wang, Y.; Wang, P.; Li, Q.X.; Guo, S.; Yan, G. Catalytic ozonation of petroleum refinery wastewater utilizing Mn-Fe-Cu/Al_2O_3 catalyst. *Environ. Sci. Pollut. Res.* **2015**, *22*, 5552–5562. [CrossRef] [PubMed]

52. Hamied, R.S.; Sukkar, K.A.; Majdi, H.S.; Shnain, Z.Y.; Graish, M.S.; Mahmood, L.H. Catalytic-level identification of prepared Pt/HY, Pt-Zn/HY, and Pt-Rh/HY nanocatalysts on the reforming reactions of n-Heptane. *Processes* **2023**, *11*, 270. [CrossRef]

53. Zhou, L.; Zhang, S.; Li, Z.; Liang, X.; Zhang, Z.; Liu, R.; Yun, J. Efficient degradation of phenol in aqueous solution by catalytic ozonation over MgO/AC. *J. Water Process Eng.* **2020**, *36*, 101168. [CrossRef]

54. Cao, Q.; Sang, L.; Tu, J.; Xiao, Y.; Liu, N.; Wu, L.; Zhang, J. Rapid degradation of refractory organic pollutants by continuous ozonation in a micro-packed bed reactor. *Chemosphere* **2021**, *270*, 128621. [CrossRef] [PubMed]